Journal of Pharmaceutical Analysis 9 (2019) 108–116

Contents lists available at ScienceDirect

Journal of Pharmaceutical Analysis

journal homepage: www.elsevier.com/locate/jpa
www.sciencedirect.com

Original Article

Controlled delivery of ibuprofen from poly(vinyl alcohol)–poly (ethylene glycol) interpenetrating polymeric network hydrogels

Subhraseema Das, Usharani Subuddhi *

Department of Chemistry, National Institute of Technology Rourkela, Rourkela 769008, Odisha, India

ARTICLE INFO

Article history:
Received 20 July 2018
Received in revised form
26 November 2018
Accepted 28 November 2018
Available online 30 November 2018

Keywords:
Hydrogels
Poly(vinyl alcohol)
Poly(ethylene glycol)
Ibuprofen
Controlled delivery systems

ABSTRACT

Hydrogels composed of poly(vinyl alcohol) (PVA) and poly(ethylene glycol) (PEG) were synthesized using glutaraldehyde as crosslinker and investigated for controlled delivery of the common anti-inflammatory drug, ibuprofen (IBF). To regulate the drug delivery, solid inclusion complexes (ICs) of IBF in β–cyclodextrin (β–CD) were prepared and added to the hydrogels. The ICs were prepared by the microwave irradiation method, which is more environmentally benign. The formation of IC was confirmed by various analytical techniques and the synthesized hydrogels were also characterized. Controlled release of drug was achieved from the hydrogels containing the ICs in comparison to the rapid release from hydrogels containing free IBF. The preliminary kinetic analysis emphasized the crucial role of β–CD in the drug release process that influences the polymer relaxation, thereby leading to prolonged release. The cytotoxicity assay validated the hydrogels as non-toxic in nature and hence can be utilized for controlled delivery of IBF.

1. Introduction

Hydrogels, as drug delivery systems, have flourished immensely in biomedical and pharmaceutical arenas in recent years. Hydrogels are three-dimensional hydrophilic polymers capable of imbibing large amounts of water or biological fluids. Fully swollen hydrogels have physical properties common to living tissues, including a soft and rubbery consistency and low interfacial tension with water or biological fluids [1,2].

Poly(vinyl alcohol) (PVA) is a common polymer widely employed in the fabrication of hydrogels intended for drug delivery purposes. PVA is endowed with good thermal and chemical stability, excellent film forming ability, long-term pH and temperature stability and high biocompatibility with living tissues [3]. In addition, PVA is non-toxic and exhibits minimal cell adhesion and protein adsorption properties [4]. However, pure PVA hydrogels are known to be quite fragile in nature. PVA hydrogels have also been chemically crosslinked by the use of crosslinking agents or radiation such as electron beams or γ-radiation in order to improve their mechanical integrity [5]. The most common strategy to overcome this limitation is to incorporate PVA into an interpenetrating polymeric network (IPN) hydrogel in combination with another polymer. PVA has been integrated with a variety of polymers to generate a wide array of hydrogels, and poly(ethylene glycol) (PEG) is one such polymer, which finds a special mention in this context. PEG is a well-favoured biomaterial due to its hydrophilicity, biocompatibility, biodegradability and elimination via both renal and hepatic pathways [6]. It has also been reported to exhibit barrier properties against bacteria and reduce cell and protein adsorption properties. Therefore, PEG hydrogels find great utility in drug delivery application, tissue engineering and regenerative medicine [7–9]. PVA-PEG hydrogels have been employed to heal acute burn wounds and also as drug delivery agents [10–12].

However, as drug delivery carriers, the major drawback that is inevitably associated with hydrogels is the inefficacy to control the initial burst release of drugs. For many medications, the burst release has been known to cause patient non-compliances. Further, the burst release is a wasteful process since too high a burst will lead to loss in effectiveness both therapeutically and economically [13]. Microencapsulation of drug is one such technology which reduces dosing frequency, resulting in a reduced concentration of free drug, thus improving patient compliances [14]. Cyclodextrins (CDs) are of special interest in this regard given their amphiphilic nature. The hydrophobic cavity is suitable for the encapsulation of a variety of guest molecules including drugs. Complexation of drug with CDs has proven to enhance the various physico-chemical properties of the drug. CDs also serve as multifunctional drug delivery carriers through the formation of inclusion complexes (ICs) [15].

In the present study, ibuprofen (IBF), a common non-steroidal anti-inflammatory drug (NSAID), has been employed to explore its

Peer review under responsibility of Xi'an Jiaotong University.
* Corresponding author.
E-mail address: subuddhiu@nitrkl.ac.in (U. Subuddhi).

https://doi.org/10.1016/j.jpha.2018.11.007

controlled release characteristics from PVA-PEG hydrogels. As such, the efficacy of IBF is hindered therapeutically due to its poor aqueous solubility and low bioavailability [16]. Complexation of IBF with β-cyclodextrin (β-CD) has proven to significantly improve its aqueous solubility, bioavailability and dissolution properties [17–19]. Solid ICs of IBF with β-CD was prepared by the novel approach of microwave irradiation method which utilizes minimal solvent, less reaction time and is more environmentally benign. The formation of IC of IBF with β-CD has been confirmed from various analytical studies. To regulate the amount of IBF released from the hydrogels, the preformed IC was added directly into the hydrogels. The hydrogels were characterized by various spectroscopic techniques. Their swelling behaviour was also investigated. The sustained drug release behaviour of the hydrogels was inspected and the preliminary kinetics has been addressed.

2. Experimental

2.1. Materials

PVA (M_w = 85,000–124,000; 86%–89% hydrolyzed) was purchased from S. D. Fine Chem., India. β-CD and IBF were procured from Sigma-Aldrich, India. PEG 4000 (M_w = 35,000–40,000; viscosity (25% aq. at 20 °C = 12 cP) was received from SRL, India. Glutaraldehyde (GA) (25%, w/v) was supplied by Spectrochem Pvt. Ltd., Mumbai, India. Milli-Q water was utilized throughout.

2.2. Preparation of solid ICs (IBF-β-CD)

The solid ICs of IBF and β-CD were prepared by the microwave irradiation method as per reported procedure [20]. Briefly, 1:1 homogeneous mixture of IBF and β–CD was taken and dissolved in minimum amounts of water-ethanol mixture (1:1, v/v). The mixture was then subjected to microwave irradiation in a scientific microwave oven (Sineo UWave-1000) at a power of 300 W for 90 s at 60 °C. The product obtained was washed with water-ethanol mixture to remove the residual IBF and β–CD and then dried under vacuum.

A physical mixture (PM) of the drug and β-CD was also prepared by homogenous blending of previously weighed 1:1 drug and β-CD in a mortar for 15 min.

2.3. Synthesis of PVA-PEG hydrogels

10% (w/v) PVA was dissolved in water by heating at 80 °C for 6 h. Requisite amounts of PEG was added to the PVA solution. To the PVA-PEG solution, GA as crosslinker and concentrated HCl as catalyst were added followed by the addition of IBF or the IBF–β–CD IC. The mixture was stirred briefly at 250 rpm at room temperature. The solution was then poured onto a clean and dried glass petri dish of known surface area to obtain a film. Hydrogel films without adding the free IBF or the IC were also synthesized in a similar fashion for comparison. The various film compositions are shown in Table 1.

Table 1
Composition and designation of synthesized hydrogels.

Sample	PVA (%, w/v)	PEG (%, w/v)	GA (%, v/v)	PVA-PEG-ibuprofen	PVA-PEG-inclusion complex
HG1	10	1	0.05	HG1-IBF	HG1-IC
HG2	10	2	0.05	HG2-IBF	HG2-IC
HG3	10	3	0.05	HG3-IBF	HG3-IC
HG4	10	4	0.05	HG4-IBF	HG4-IC
HG5	10	5	0.05	HG5-IBF	HG5-IC

2.4. Instruments used for characterization

2.4.1. Fourier Transformed Infrared Spectroscopy (FTIR)

The FTIR spectra were analyzed in a Perkin Elmer RX I FTIR spectrophotometer. The samples were mixed with dry KBr and compressed into pellets and scanned from 4000 to 400 cm^{-1}.

2.4.2. X-Ray diffraction (XRD)

XRD profiles of the samples were collected on a PANalytical X-Ray diffractometer using Nickel-filtered Cu K_α radiation and scanned from 5° to 40° at room temperature at a scan rate of 3°/min.

2.4.3. Differential Scanning Calorimetry (DSC)

DSC was performed by Netzsch DSC200 instrument on 5–10 mg of samples and scanned in perforated Al-pans under N_2 atmosphere (purging rate: 40 mL/min) in the 50–150 °C temperature range at a heating rate of 10 °C/min. The DSC of dried hydrogel samples weighing 1–5 mg was taken in Al-crucibles and sealed with Al-lid. All the samples were first heated over the temperature range from 25 °C to 150 °C (first heating cycle), and then cooled to 25 °C followed by heating again up to 250 °C (second heating cycle), at a heating rate of 10 °C/min under N_2 atmosphere (purging rate: 40 mL/min).

2.4.4. Scanning Electron Microscopy (SEM)

The SEM micrographs of the samples were observed on a JEOL SEM, JSM 6480LV model. The hydrogels were first swollen in water till equilibrium and then lyophilized in a Scanvac lyophilizer at − 55 °C for 48 h. The samples were sputtered coated with gold and then observed under SEM.

2.4.5. ^{1}H Nuclear Magnetic Resonance (NMR)

^{1}H NMR spectrum was performed using a Bruker 400 MHz NMR spectrometer in D_2O obtained from Sigma-Aldrich, India.

2.5. Swelling properties of hydrogels

The swelling behaviour of the hydrogels was investigated by immersing them in phosphate buffer solution (pH = 7.4) at 37 °C. Samples were taken out at certain intervals and weighed after removing the surface water by gentle wiping with filter paper. The swollen gel was then slowly dried to constant weight. The swelling percentage was calculated according to the following formula [21]:

$$Swelling(\%) = \frac{W_s - W_d}{W_d} \times 100 \quad (1)$$

where W_s and W_d are the weights of the swollen and dried hydrogels, respectively. All experiments were carried out in triplicate and the mean data were presented.

2.6. In vitro drug release studies

In vitro release studies of the drug was carried out by placing the drug loaded hydrogels in 50 mL of the releasing medium at 37 °C and taking out aliquots of 3 mL at particular time intervals. The amount of drug released from the hydrogels was determined spectrophotometrically at λ_{max} = 276 nm for IBF in a Shimadzu UV–Vis spectrophotometer (UV-1800). The withdrawn aliquots were replenished with equal volumes of phosphate buffer solution to simulate physiological conditions. The sink conditions were maintained throughout the scope of the release study. The concentration of drug released was estimated from the calibration plot of IBF. The release data were expressed as the mean value of three independent experiments and the standard deviations were also

presented as error bars. The results have been presented in terms of percentage release as a function of time using the following formula [22]:

$$\text{Cumulative release}(\%) = \frac{W_t}{W_l} \times 100 \quad (2)$$

where W_t is the amount of drug released from hydrogel at time t and W_l is the amount of drug loaded onto the hydrogel.

2.7. Drug release kinetics

The probable mechanism of drug release from the hydrogels was investigated by analyzing the release data according to four basic empirical mathematical equations. All these equations hold good only for the first 60% of drug release [23]. The data were analyzed using OriginPro 7 (OriginLab Corporation).

Model 1: Higuchi equation that describes the Fickian diffusion of a drug [24]:

$$M_t/M_\infty = k \cdot t^{0.5} \quad (3)$$

Where, M_t/M_∞ is the fractional drug release, k is a kinetic constant, and t is the release time.

Model 2: Ritger–Peppas equation [25]:

$$M_t/M_\infty = k' \cdot t^n \quad (4)$$

Where k' is a kinetic constant, t is the release time, and n is the diffusional exponent that can be related to the drug transport mechanism. For a thin hydrogel film, when $n = 0.5$, the drug release mechanism is Fickian diffusion, which occurs by the usual molecular diffusion of the drug due to a chemical potential gradient. When $n = 1$, Case II transport occurs, which is associated with the relaxational release of drug leading to zero-order kinetics. When the value of n is between 0.5 and 1, anomalous transport is observed where both Fickian and relaxational phenomena contribute to the drug release.

Model 3: Peppas–Sahlin equation accounting for the coupled effects of Fickian diffusion and Case II transport [26]:

$$M_t/M_\infty = k_1 \cdot t^m + k_2 \cdot t^{2m} \quad (5)$$

The first term on the right hand side of this equation represents the contribution of Fickian diffusion and the second term refers to the macromolecular relaxation contribution on the overall release mechanism. k_1 is the diffusion constant and k_2 is the relaxation rate constant. The coefficient m is the Fickian diffusion exponent that depends on the geometry of the device. For thin films, the value of m is 0.5.

Using the estimated parameters k_1 and k_2, the ratio of relaxation (R) and Fickian (F) contributions was calculated using Eq. (6) as:

$$R/F = (k_2/k_1)t^m \quad (6)$$

Model 4: Zero-order kinetics

$$M_t/M_\infty = k'' \cdot t \quad (7)$$

where k'' is the zero-order kinetic rate constant.

2.8. Cytotoxicity assay

Cytotoxicity assay of the prepared hydrogels was performed by MTT colorimetric technique using 9 mm diameter discs of the hydrogel films. Prior to the assay, the hydrogels were sterilized at 15 lb/in^2 steam pressure, 121 °C for 1 h. The cytotoxicity was evaluated by using L929NCCS rat fibroblast cell line. The cell growth was performed on a 24-well tissue culture plate in a controlled atmosphere (5% CO_2 at 37 °C) using a cell culture medium of Dulbecco's Modified Eagle's Medium (DMEM, Hi-Media, India) supplemented with 10% Fetal Bovine Serum (FBS, Hi-Media, India) and penicillin–streptomycin antibiotic solution (Hi-Media, India). 90% of confluent monolayers of cultured cells were harvested by trypsinization (0.25% Trypsin and 0.02% EDTA, Hi-Media, India) and 1 mL of 1 × 10^{5}cells/mL were seeded in each

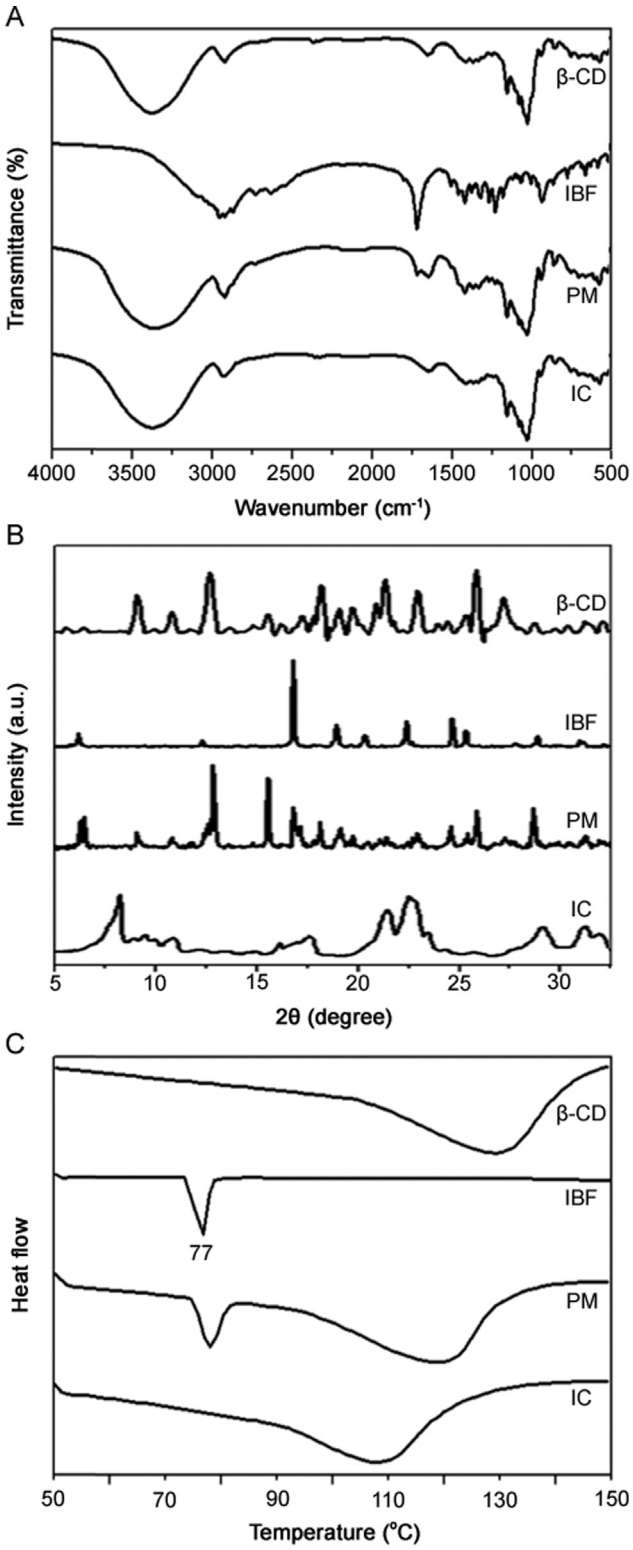

Fig. 1. (A) FTIR spectra, (B) XRD profiles and (C) DSC thermograms of β-CD, IBF, PM and IC.

well. The culture plate was then incubated for 48 h in the CO_2 incubator at 37 °C. The cytotoxicity analysis was performed as per standard protocol.

3. Results and discussion

3.1. Inclusion of IBF into β-CD cavity

The inclusion phenomenon of IBF with β-CD was confirmed from various analytical techniques, the details of which are presented below.

3.1.1. FTIR analysis

FTIR is a useful technique to study the formation of ICs because the characteristics peaks of the guest molecules generally shift or disappear upon inclusion in host cavity [27]. The FTIR spectrum of β-CD (Fig. 1A) shows the characteristic peaks which include the broad band with a maximum at 3377 cm^{-1} due to the stretching vibrations of the hydroxyl groups, an absorption band at 2917 cm^{-1} attributed to the C-H stretching, a band at 1647 cm^{-1} assigned to the bending vibrations of O-H bonds in COH groups and/or in water molecules and a band at 1412 cm^{-1} owing to the bending vibration of C-H bonds in CH_2OH and CHOH groups [28]. The FTIR spectrum of IBF shows the presence of a band at 1724 cm^{-1} corresponding to the carbonyl stretching. The PM exhibited both the features of β-CD and IBF. However, the drug peak due to carbonyl stretching vibration disappeared in the FTIR spectra of the IC. Also, O-H_{str} peak at 3377 cm^{-1} and C-H_{str} at 2917 cm^{-1} observed in the spectra of β-CD shifted to 3387 cm^{-1} and 2938 cm^{-1} in that of the IC. These spectral modifications indicate the inclusion of IBF into the β-CD cavity and the formation of an IC [18].

3.1.2. XRD analysis

Formation of IC is indicated by the appearance of new or modified peaks from the original XRD patterns. Fig. 1B displays the powder XRD patterns of β-CD, IBF, PM and IC. The XRD profile of β-CD and IBF exhibited numerous distinct peaks that clearly points towards their crystalline nature. The principal peaks from IBF and β-CD were present in the diffractogam of PM. But the diffraction profile of IC presented a completely different pattern with new peaks, which indicated the formation of an IC [29].

3.1.3. DSC analysis

DSC is usually employed as an important tool to affirm the formation of IC of β-CD with guests. The DSC thermograms of β-CD, IBF, PM and IC are presented in Fig. 1C. The DSC curve of β-CD showed a broad endothermic effect around 120 °C which is associated with its dehydration process. The thermogram of IBF was typical of a crystalline anhydrous substance with a sharp peak at 77 °C, indicating its melting point. For the PM, the endotherms corresponding to the dehydration of β-CD and melting of IBF were observed. The DSC curve for the IC revealed the disappearance of the IBF melting point and only the peak from β-CD was observed. These results signified the inclusion of IBF into β-CD cavity [29].

3.1.4. SEM analysis

Fig. 2A illustrates the SEM images of β-CD, IBF, PM and IC captured at a voltage of 5.00 kV and 100× magnification. The particles of β–CD were found to be crystalline type with different dimensions and polyhedral in nature. The particles of IBF were found to be rod-shaped. The PM comprised of morphology of both β–CD and IBF. However, IC presented a total different morphology. They were found to be block-types with smaller dimensions, unlike the morphologies of either β–CD or IBF. This morphological difference in β–CD, IBF and IC substantiates the formation of new entities of ICs.

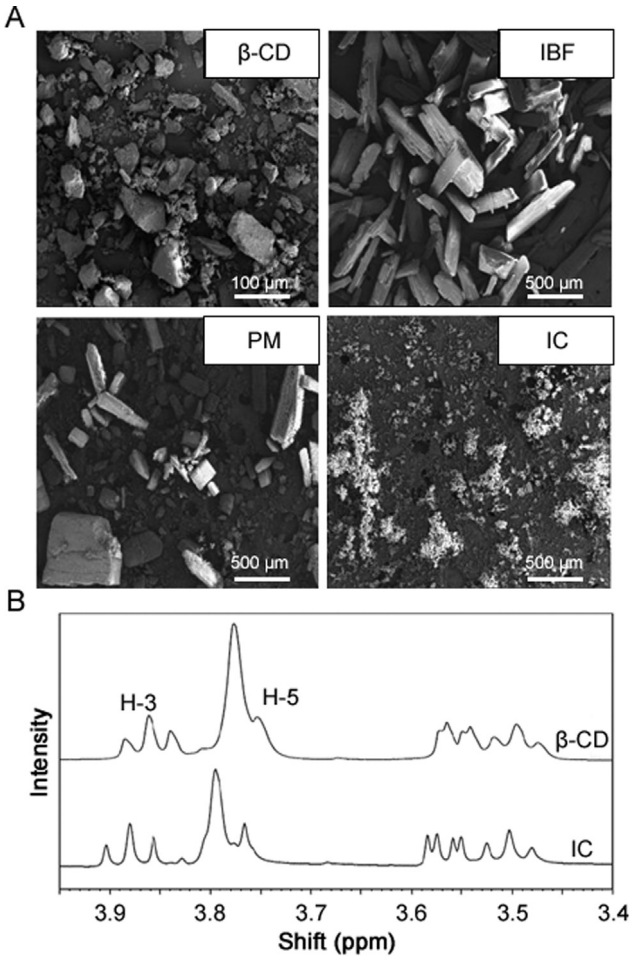

Fig. 2. (A) SEM images of β-CD, IBF, PM, IC, and (B) ^{1}H NMR spectra of β-CD and IC in D_2O at 25 °C.

3.1.5. ^{1}H NMR analysis

^{1}H NMR provides direct evidence for the formation of ICs (drug-β-CD). β-CD has the topology of a hollow cone with H-3 and H-5 being the inner protons. The hydrophobic guests get included in the toroidal cavity of β-CD, thereby affecting its inner protons. The changes in the chemical shifts of H-3 and H-5 protons of β-CD and IC suggest the inclusion process. When $[\Delta(\delta H3) > \Delta(\delta H5)]$, the inclusion of the guest inside the cavity is partial while $[\Delta(\delta H3) \leq \Delta(\delta H5)]$ indicates total inclusion of guest inside β-CD cavity [30]. The ^{1}H NMR spectra of β-CD and IC are shown in Fig. 2B.

The positions of H-3 and H-5 protons were calculated in the IC and found to be shifted *ca.* 0.058 ppm and 0.086 ppm in IC with respect to the native β-CD. Since $\Delta(\delta H3) < \Delta(\delta H5)$, total inclusion of IBF into β-CD cavity has occurred.

3.2. Characterization of hydrogels

3.2.1. FTIR analysis

The FTIR spectra of neat PVA, PEG and the HG5 IPN hydrogel are shown in Fig. 3A. The characteristic peaks of PVA include a large band at 3400 cm^{-1} (O–H stretch), the peaks at 2935 cm^{-1} (C–H stretch from alkyl groups), 1720 cm^{-1} (C═O stretch) and 1140 cm^{-1} (C═O stretch of semi-crystalline PVA). The peaks at 1280, 950 and 843 cm^{-1} in the spectra of PEG are due to its crystalline regions [31]. In the HG5 hydrogel, the characteristic peaks of PVA and PEG are seen with a small shift in their frequencies. The semi-crystalline peak of PVA at 1140 cm^{-1} and the

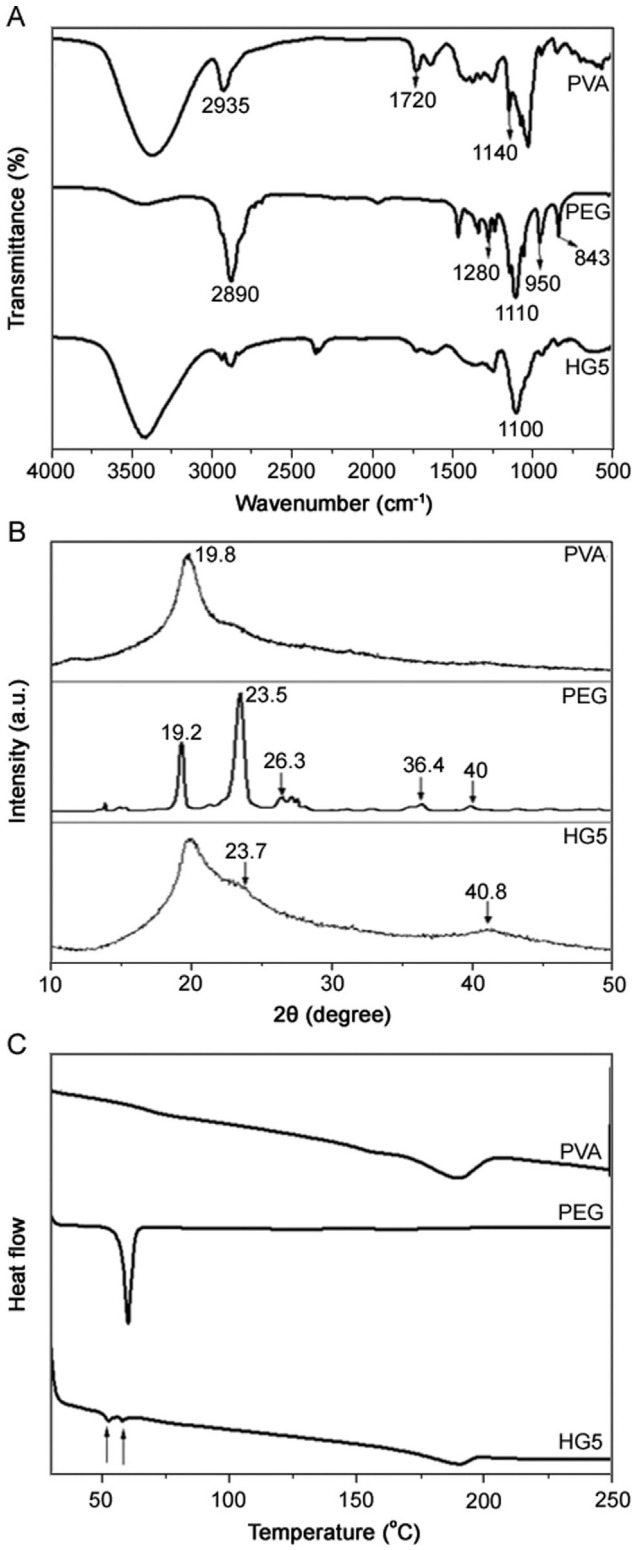

Fig. 3. (A) FTIR spectra, (B) XRD profiles and (C) DSC thermograms of neat PVA, neat PEG and HG5 hydrogel.

crystalline peaks of PEG are altogether absent in the FTIR spectral profile of HG5, indicating the loss in the regularity of PVA and PEG polymer chains due to interpolymer interaction.

3.2.2. XRD analysis

The XRD profiles of neat PVA, PEG and the HG5 IPN hydrogel are illustrated in Fig. 3B. PVA exhibits a peak at diffraction angle 2θ of 19.8°, indicating its semi-crystalline nature [32]. The diffraction profile of PEG suggests its crystalline nature with strong reflections at 19.2° and 23.5° and weak reflections at 26.3°, 36.4° and 40° owing to its close molecular packing and regular crystallization [33]. From the XRD patterns of the HG5 IPN hydrogels, it could be seen that diffraction peaks appeared at around 19° and 23° with increasing PEG content. This can be explained by the strong interaction between PVA and PEG which has destroyed close packing of PVA molecules for the formation of regular crystallites and also has created new crystallites [34]. In other words, the results of XRD analysis reinforce the existence of good compatibility between the parent polymers in the resulting IPNs.

3.2.3. DSC analysis

Fig. 3C shows the DSC thermograms of neat PVA, PEG and the HG5 IPN hydrogel. Neat PVA exhibited a melting temperature (T_m) at around 190 °C and that for PEG was observed at around 56 °C [32,35]. For the DSC curve of the HG5 IPN hydrogel, the peak at 190 °C was due to the melting of PVA. Moreover, two peaks are also present at 56 °C and 60 °C temperature scales which conform to the melting of PEG. It can be inferred that as PEG content is increased in the IPN hydrogels, PVA chains inhibit the crystallization of PEG where the interface between these polymers acts as a crystal nucleus for PEG crystallinity, which is referred to as heterogeneous nucleation-induced crystallization [12]. It is known that homogeneous nucleation-induced crystallization also occurs in the hydrogel matrix if the amount of PVA is insufficient in the matrix for nucleation. This particular multi-crystallizability enhances the interaction between the two polymers leading to improved mechanical integrity of the resulting HG5 IPN hydrogel [12,36].

3.2.4. SEM analysis

The morphology of the hydrogels was studied by SEM and the images are presented in Fig. 4. As evident, the HG1 hydrogel possesses a highly porous network structure. The porosity of the hydrogels gradually decreases with the increase in PEG content in the matrix. This is clearly seen from the above images. This increased matrix density could be attributed to enhanced entanglements in the hydrogel matrix due to enhanced interpolymer interaction. The HG4 and HG5 hydrogels exhibited the densest and most rigid matrix structures among all the synthesized hydrogels probably due to higher amounts of PEG in their matrices. Similar results have been reported earlier for PVA-PEG hydrogels and the thicker matrix density with increasing PEG has been attributed to the accumulation of PEG around the PVA backbone and cavities in the network [12].

3.3. Swelling response of hydrogels

Swelling is a crucial parameter to characterize hydrogels to determine their drug releasing property. The equilibrium swelling profiles of HG1, HG2, HG3, HG4 and HG5 hydrogels as a function of time were studied and the data are displayed in Fig. 5.

A gradual decrease in the degree of swelling was observed with increased PEG content in the hydrogels. This can be rationalized by considering the morphological dependence of these hydrogels on the PEG amount. As evident from the SEM studies, HG1, HG2 and HG3 hydrogels are porous in nature and therefore can accommodate more water in their capillary pores, resulting in higher swelling ability. The decrease in swelling in HG4 and HG5 hydrogels could be due to the increased matrix density, which restricted the inward flow of solvent molecules. The HG5 hydrogel showed the lowest swellability among all.

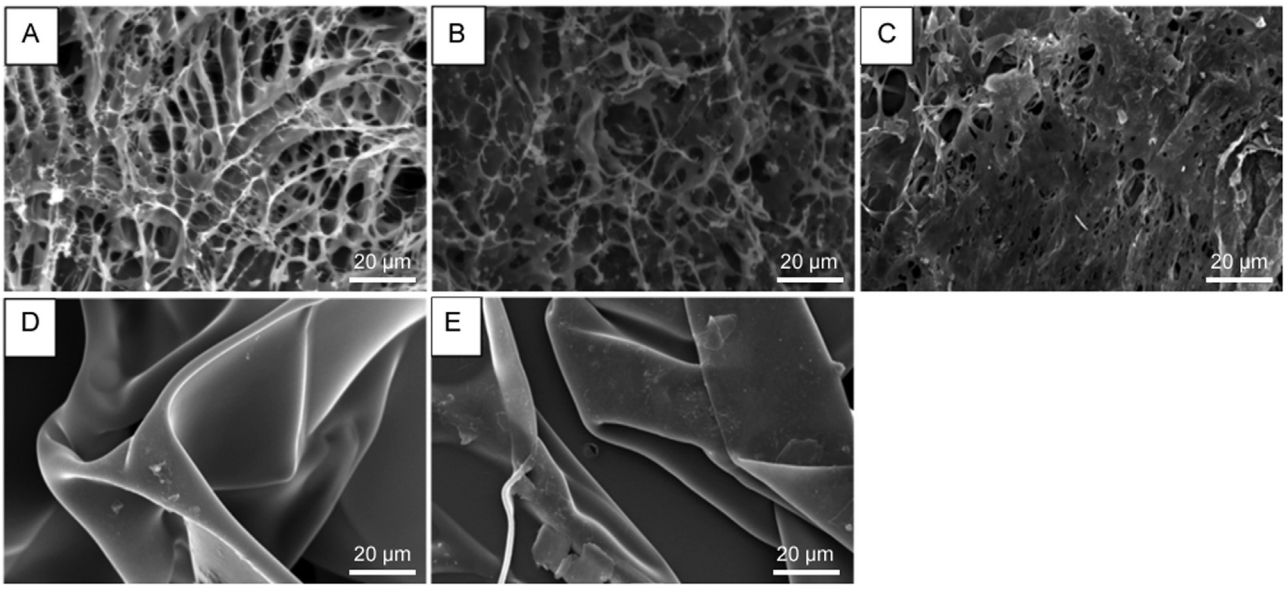

Fig. 4. SEM images of (A) HG1, (B) HG2, (C) HG3, (D) HG4 and (E) HG5 hydrogels.

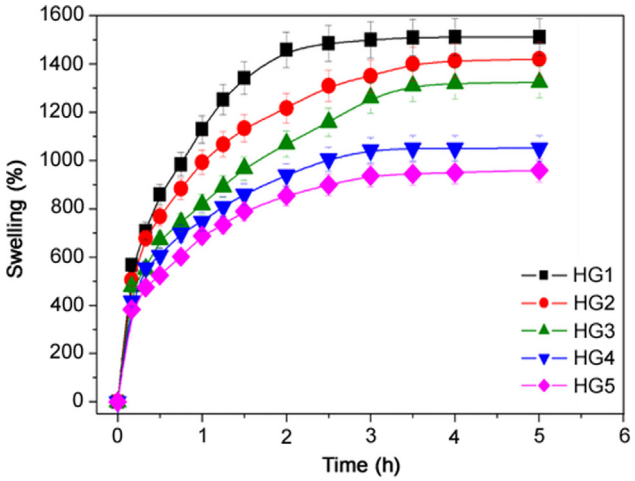

Fig. 5. Swelling profiles of HG1, HG2, HG3, HG4 and HG5 hydrogels in pH 7.4 buffer at 37 °C.

3.4. *In vitro IBF release studies and kinetics*

Prior to drug release studies, IBF content in the IC was estimated, which agreed well with the theoretical value (≈ 16%). In our case, we have taken 10 mg of IBF and equivalent amount of IBF-β-CD IC (containing 10 mg of IBF) and assayed the drug content spectrophotometrically at $\lambda_{max} = 276$ nm. IBF release profiles from HG-IBF and HG-IC hydrogels are illustrated in Figs. 6A and B, respectively. As seen, drug release from HG-IBF hydrogels takes place rapidly. However, IBF release from HG-IC hydrogels is much slower and occurs over a prolonged period of time. This difference in release rates of IBF can be rationalized by considering the modes of drug diffusion from these two hydrogel matrices. Since the drug is freely dispersed in the HG-IBF hydrogels, drug release occurs as the drug molecule diffuses out of the hydrogel matrix. On the other hand, IBF is present in an IC with β-CD in the HG-IC hydrogels. The presence of the drug in an IC form offers an additional diffusion barrier that results in its slow diffusion from the hydrogel matrix. An important factor that needs to be brought to notice in this context is the high binding constant of IBF with β–CD ($\approx 10^3\ M^{-1}$) [37,38]. In this study the $K_{1:1}$ for IBF–β–CD IC was also

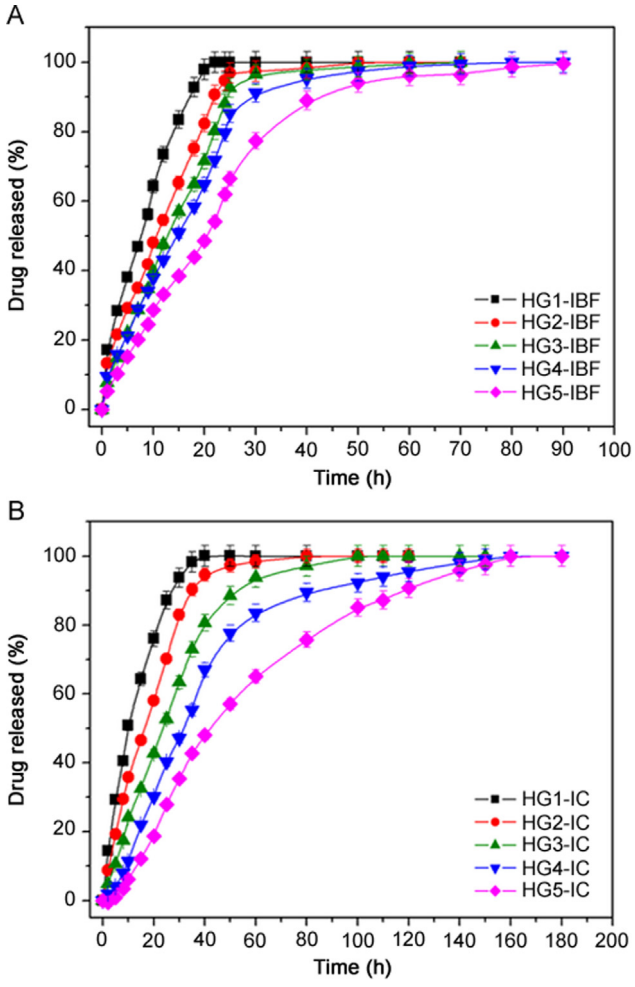

Fig. 6. IBF release profiles from (A) HG1-IBF, HG2-IBF, HG3-IBF, HG4-IBF, and HG5-IBF, and (B) HG1-IC, HG2-IC, HG3-IC, HG4-IC, and HG5-IC hydrogels in pH 7.4 buffer at 37 °C.

calculated according to the modified Benesi-Hilberband equation [37,38] and it was found to be in close proximity with the reported values. Stronger is the binding of the drug with β–CD, slower is its

Table 2
Fitting parameters for release data obtained from various mathematical models.

Sample	Higuchi		Ritger–Peppas			Peppas-Sahlin			Zero-Order	
	k ($h^{-0.5}$)	R^2	n	k' (h^{-n})	R^2	k_1 ($h^{-0.5}$)	k_2 (h^{-1})	R^2	k'' (h^{-1})	R^2
HG1-IBF	0.348	0.976	0.56	0.335	0.994	0.304	0.031	0.981	0.235	0.738
HG2-IBF	0.287	0.947	0.69	0.238	0.997	0.158	0.079	0.998	0.171	0.925
HG3-IBF	0.248	0.901	0.83	0.174	0.999	0.074	0.100	0.998	0.141	0.981
HG4-IBF	0.196	0.863	0.94	0.116	0.998	0.023	0.094	0.998	0.107	0.906
HG5-IBF	0.165	0.889	0.86	0.108	0.996	0.042	0.067	0.997	0.09	0.985
HG1-IC	0.243	0.865	0.85	0.158	0.997	0.066	0.094	0.995	0.128	0.978
HG2-IC	0.156	0.676	0.84	0.078	0.994	−0.071	0.135	0.987	0.094	0.958
HG3-IC	0.166	0.754	0.88	0.063	0.981	0.028	0.085	0.982	0.073	0.978
HG4-IC	0.161	0.833	0.91	0.071	0.990	0.021	0.051	0.988	0.058	0.984
HG5-IC	0.122	0.777	0.92	0.038	0.984	−0.012	0.045	0.985	0.041	0.983

k: Fickian diffusion kinetic constant, n: diffusional exponent, k': kinetic constant in the Ritger-Peppas equation, k_1 is the diffusion and k_2 is the relaxation rate constant in the Peppas-Sahlin equation, k'': zero-order kinetic rate constant, R^2: fitting parameter.

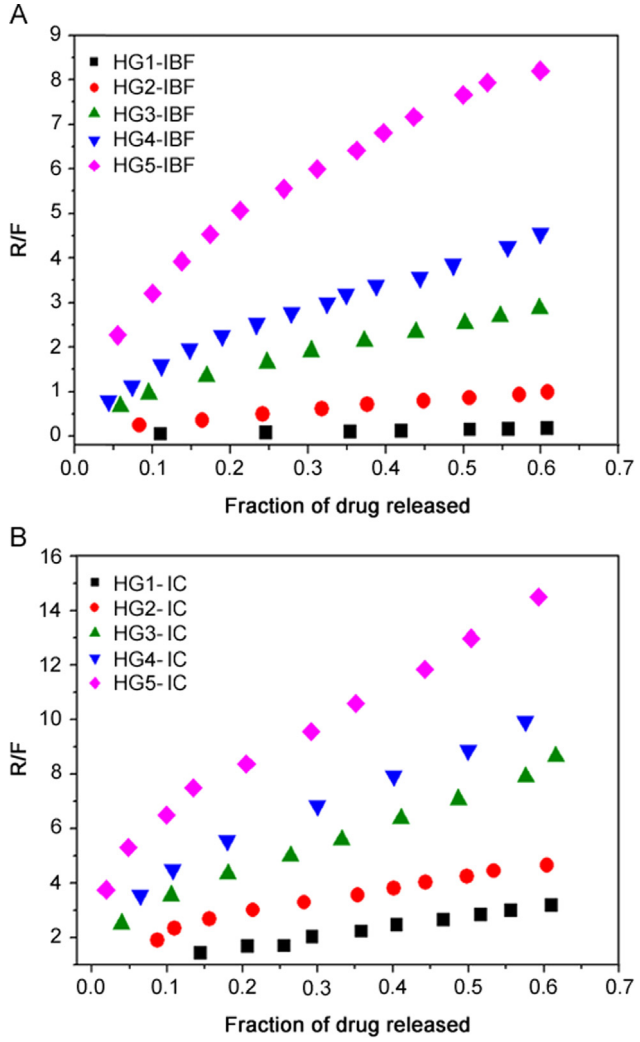

Fig. 7. Plots of R/F versus the fraction of drug released from (A) HG1-IBF, HG2-IBF, HG3-IBF, HG4-IBF, HG5-IBF, and (B) HG1-IC, HG2-IC, HG3-IC, HG4-IC, HG5-IC hydrogels.

release from β–CD cavity. Thus the diffusivity of the drug from HG-IC hydrogels slows due to an additional diffusion barrier imposed by β–CD leading to an extended release.

The rate of drug release from the hydrogels was found to decrease in the order of HG1 > HG2 > HG3 > HG4 > HG5, irrespective of the hydrogel containing IBF or IC. However, at any time, the amount of IBF released was always less in case of the hydrogels containing the ICs. The HG5-IC hydrogel was found the best of the lot with the slowest drug releasing characteristics.

3.5. Drug release kinetics

Table 2 summarizes the kinetic parameters for the drug release data analyzed according to four basic empirical equations, which provides an approximate idea about the drug transport mechanism.

It was found that the IBF release data showed the best fit to the Ritger-Peppas and Peppas-Sahlin equations in almost all the cases. The values of the diffusional exponent (n) lie between 0.56 and 0.94, indicating the anomalous nature of drug release, where both diffusion and relaxation processes contribute. It is not possible to know exactly the contribution of these two processes from the estimated values of k_1 and k_2 alone; hence the ratio of the relaxational over Fickian contributions (R/F) was calculated for the samples and plotted against the fraction of the drug released from the hydrogels (Fig. 7).

The R/F value increased in the order of HG5 > HG4 > HG3 > HG2 > HG1, irrespective of whether the hydrogels contain IBF or IC. This can be explained by considering that with increased PEG content, the hydrogel matrix changes from a porous organization to a rigid and denser structure which affects the polymer relaxation, thereby influencing the drug release mechanism. The R/F values for HG1-IBF, HG2-IBF, HG3-IBF, HG4-IBF, and HG5-IBF were found to be lower than those of the corresponding HG1-IC, HG2-IC, HG3-IC, HG4-IC and HG5-IC hydrogels, respectively. This

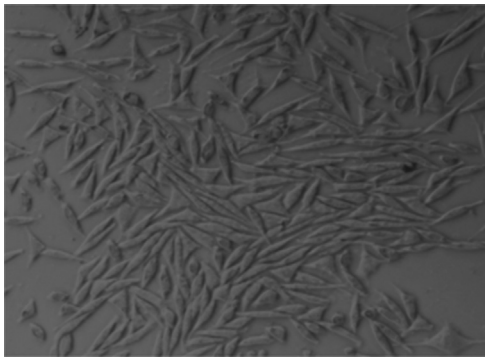

Fig. 8. Optical micrograph of fibroblast cells cultured with HG5 hydrogel after 48 h of incubation.

indicated that the presence of β–CD also influences the relaxation rate of the polymers, which leads to prolonged release of IBF from the IC-containing hydrogels. This is further supported by the presence of hydrogen bonding interaction between β–CD and the polymers or β–CD getting crosslinked to some extent in the presence of GA [39,40]. Among all the films, the relaxation contribution was found to be the maximum for HG5-IC hydrogel.

3.6. Cytotoxicity assay

While designing a material for biomedical purposes, it is of utmost importance to characterize it in terms of biocompatibility. The biocompatibility of HG5 hydrogel was performed by MTT colorimetric technique. As shown in Fig. 8, direct contact between L929 cells and the hydrogel did not reveal any adverse effect. This suggests the high compatibility and non-toxicity of the hydrogel with the living tissues, thus validated as potential drug delivery systems.

4. Conclusion

Hydrogels comprising poly(vinyl alcohol) (PVA) and poly (ethylene glycol) (PEG) were synthesized using glutaraldehyde as crosslinker and investigated for controlled delivery of the common NSAID, ibuprofen (IBF). To regulate the drug delivery, solid IC of IBF with β–CD was prepared by the novel approach of microwave irradiation method and added to the hydrogels. The formation of ICs of IBF in β–CD was confirmed by various analytical techniques. The synthesized hydrogels were also characterized by FTIR, XRD, DSC and their morphology inspected. The XRD and DSC studies revealed that the two polymers exhibited good compatibility in the resulting IPNs. The swelling studies indicated that swellability of the hydrogels decreased with an increase in the PEG content. Controlled release of drug was achieved from the hydrogels containing the ICs in comparison to the rapid release from hydrogels containing free IBF. The rate of drug release was found to decrease with an increase in the PEG content in the hydrogels. The preliminary kinetic analysis emphasized the crucial role of β–CD in the drug release process that influences the polymer relaxation, thereby leading to prolonged release. Further analysis of R/F values suggested the presence of hydrogen bonding interaction between β–CD and the polymers or β–CD getting crosslinked to some extent in the presence GA, thereby influencing the macromolecular relaxation. Among all the films, the HG5-IC hydrogel was found to be the best of the lot for controlled delivery of ibuprofen.

Conflicts of interest

The authors declare that there are no conflicts of interest.

References

[1] T.R. Hoare, D.S. Kohane, Hydrogels in drug delivery: Progress and challenges, Polymer 49 (2008) 1993–2007.
[2] N.A. Peppas, P. Bures, W. Leobandung, et al., Hydrogels in pharmaceutical formulations, Eur. J. Pharm. Biopharm. 50 (2000) 27–46.
[3] D.S. Deshpande, R. Bajpai, A.K. Bajpai, Synthesis and characterization of polyvinyl alcohol-based semi interpenetrating polymeric networks, J. Polym. Res. 19 (2012) 9938.
[4] C.M. Hassan, N.A. Peppas, Structures and applications of poly (vinyl alcohol) hydrogels produced by conventional crosslinking or by freeze/ thawing methods, in: A. Abe, A.-C. Albertsson, H.-J. Cantow, et al., (Eds.), Biopolymers PVA Hydrogels, Anionic Polymerisation Nanocomposites, Adv. Polym. Sci., Springer-Verlag, Berlin Heidelberg, New York, 2000, pp. 37–65.
[5] W. Li, F. Xue, R. Cheng, States of water in partially swollen poly (vinyl alcohol) hydrogel, Polymer 46 (2005) 12026–12031.
[6] F.M. Veronese, G. Pasut, PEGylation, successful approach to drug delivery, Drug Discov. Today 10 (2005) 1451–1458.
[7] M. Parlato, S. Reichert, N. Barney, et al., Poly(ethylene glycol) hydrogels with adaptable mechanical and degradation properties for use in biomedical applications, Macromol. Biosci. 14 (2014) 687–698.
[8] C.-C. Lin, K.S. Anseth, PEG hydrogels for the controlled release of biomolecules in regenerative medicine, Pharm. Res. 26 (2009) 631–643.
[9] Q. Wang, N. Zhang, X. Hu, et al., Alginate/polyethylene glycol blend fibers and their properties for drug controlled release, J. Biomed. Mater. Res. A 82 (2007) 122–128.
[10] P.J. Martens, S.J. Bryant, K.S. Anseth, Tailoring the degradation of hydrogels formed from multi vinyl poly(ethylene glycol) and poly(vinyl alcohol) macromers for cartilage tissue engineering, Biomacromolecules 4 (2003) 283–292.
[11] A. Gupta, N.K. Upadhyay, S. Parthasarathy, et al., Nitrofurazone loaded PVA-PEG semi-IPN for application as hydrogel dressing for normal and burns wound, J. Appl. Polym. Sci. 128 (2013) 4031–4039.
[12] X. Zhang, X. Guo, S. Yang, et al., Double-network hydrogel with high mechanical strength prepared from two biocompatible polymers, J. Appl. Polym. Sci. 112 (2009) 3063–3070.
[13] X. Huang, C.S. Brazel, On the importance and mechanisms of burst release in matrix-controlled drug delivery systems, J. Control. Release 73 (2001) 121–136.
[14] K.M. Manjanna, B. Shivakumar, T.M. Pramod Kumar, Microencapsulation: An acclaimed novel drug-delivery system for NSAIDS in arthritis, Crit. Rev. Ther. Drug Carr. Syst. 27 (2010) 509–545.
[15] A. Vyas, S. Saraf, S. Saraf, Cyclodextrin based novel drug delivery systems, J. Incl. Phenom. Macrocycl. Chem. 62 (2008) 23–42.
[16] J.D. Higgins, T.P. Gilmor, S.A. Martellucci, et al., Ibuprofen, in: H.G. Brittain (Ed.), Analytical Profiles of Drug Substances and Excipients, 27, Academic Press, London, 2001, pp. 265–300.
[17] T. Hladon, J. Pawlaczyk, B. Szafran, Stability of ibuprofen in its inclusion complex with β–cyclodextrin, J. Incl. Phenom. Macrocycl. Chem. 36 (2000) 1–8.
[18] P. Mura, G.P. Bettinetti, A. Manderioli, et al., Interactions of ketoprofen and ibuprofen with β–cyclodextrins in solution and in solid state, Int. J. Pharm. 166 (1998) 189–203.
[19] K. Hussein, M. Turk, M.A. Wahl, Comparative evaluation of ibuprofen/β-cyclodextrin complexes obtained by supercritical carbon dioxide and other conventional methods, Pharm. Res. 24 (2007) 585–592.
[20] D. Zhao, K. Liao, X. Ma, et al., Study of the supramolecular inclusion of β–cyclodextrin with andrographolide, J. Incl. Phenom. Macrocycl. Chem. 43 (2002) 259–264.
[21] R.V. Kulkarni, V.V. Baraskar, C.M. Setty, et al., Interpenetrating polymer network matrices of sodium alginate and carrageenan for controlled drug delivery application, Fibers Polym. 12 (2011) 352–358.
[22] M.C.I.M. Amin, N. Ahmad, N. Halib, et al., Synthesis and characterization of thermo- and pH-responsive bacterial cellulose/acrylic acid hydrogels for drug delivery, Carbohydr. Polym. 88 (2012) 465–473.
[23] L. Serra, J. Doménech, N.A. Peppas, Drug transport mechanisms and release kinetics from molecularly designed poly(acrylic acid-*g*-ethylene glycol) hydrogels, Biomaterials 27 (2006) 5440–5451.
[24] T. Higuchi, Mechanism of sustained-action medication. Theoretical analysis of rate of release of solid drugs dispersed in solid matrices, J. Pharm. Sci. 52 (1963) 1145–1149.
[25] P.L. Ritger, N.A. Peppas, A simple equation for description of solute release II. Fickianand anomalous release from swellable device, J. Control. Release 5 (1987) 37–42.
[26] N.A. Peppas, J.J. Sahlin, A simple equation for the description of solute release. III. Coupling of diffusion and relaxation, Int. J. Pharm. 57 (1989) 169–172.
[27] A.S. Priya, J. Sivakamavalli, B. Vaseeharan, et al., Improvement on dissolution rate of inclusion complex of rifabutin drug with β-cyclodextrin, Int. J. Biol. Macromol. 62 (2013) 472–480.
[28] Z.-W. Gao, X.-P. Zhao, Guest controlling effects on ER behaviors of β-cyclodextrin polymer, J. Colloid Interface Sci. 289 (2005) 56–62.
[29] P.J. Salústio, G. Feio, J.L. Figueirinhas, et al., The influence of the preparation methods on the inclusion of model drugs in β-cyclodextrin cavity, Eur. J. Pharm. Biopharm. 71 (2009) 377–386.
[30] D. Greatbanks, R. Pickford, Cyclodextrins as chiral complexing agents, in water and their application to optical purity measurements, Magn. Reson. Chem. 25 (1987) 208–215.
[31] P. Kolhe, R.M. Kannan, Improvement in ductility of chitosan through blending and copolymerization with PEG: FTIR investigation of molecular interactions,

Biomacromolecules 4 (2003) 173–180.
[32] P.R. Hari, K. Sreenivasan, Preparation of polyvinyl alcohol hydrogel through the selective complexation of amorphous phase, J. Appl. Polym. Sci. 82 (2001) 143–149.
[33] D.O. Corrigan, A.M. Healy, O.I. Corrigan, The effect of spray drying solutions of polyethylene glycol (PEG) and lactose/PEG on their physicochemical properties, Int. J. Pharm. 235 (2002) 193–205.
[34] Q. Wang, Z. Dong, Y. Du, et al., Controlled release of ciprofloxacin hydrochloride from chitosan/polyethylene glycol blend films, Carbohydr. Polym. 69 (2007) 336–343.
[35] S.E. Bartsch, U.J. Griesser, Physicochemical properties of the binary system glibenclamide and polyethylene glycol 4000, J. Therm. Anal. Calorim. 77 (2004) 555–569.
[36] S.J. Lee, S.S. Kim, Y.M. Lee, Interpenetrating polymer network hydrogels based on poly(ethylene glycol) macromer and chitosan, Carbohydr. Polym. 41 (2000) 197–205.
[37] J.L. Manzoori, M. Amjadi, Spectrofluorimetric study of host-guest complexation of ibuprofen with β-cyclodextrin and its analytical application, Spectrochim. Acta A 59 (2003) 909–916.
[38] L.A. Hergert, G.M. Escandar, Spectrofluorimetric study of β-cyclodextrin ibuprofen complex and determination of ibuprofen in pharmaceutical preparations and serum, Talanta 60 (2003) 235–246.
[39] S. Das, U. Subuddhi, Cyclodextrin mediated controlled release of naproxen from pH-sensitive chitosan/poly(vinyl alcohol) hydrogels for colon targeted delivery, Ind. Eng. Chem. Res. 52 (2013) 14192–14200.
[40] D.C. Bibby, N.M. Davies, I.G. Tucker, Mechanisms by which cyclodextrins modify drug release from polymeric drug delivery systems, Int. J. Pharm. 197 (2000) 1–11.